

---

## Potential rockfalls and analysis of slope dynamics in the Palatine archaeological area (Rome, Italy)

---

E. DI LUZIO<sup>|1|</sup> G. BIANCHI FASANI<sup>|2|</sup> A. BRETSCHNEIDER<sup>|3|</sup>

<sup>|1|</sup> **CNR-ITABC, Institute for Technologies applied to Cultural Heritage, Area della Ricerca di Roma RM 1**  
Montelibretti, Via Salaria km 29.300, C.P.10 – 00016 Monterotondo Stazione, Rome (Italy). E-mail: emiliano.diluzio@itabc.cnr.it  
Fax: 39 06 90672684

<sup>|2|</sup> **CERI Research Centre on Prevention Prediction and Control of Geological Risks. Sapienza University of Rome**  
Piazza U. Piloizzi, 9, 00038, Valmontone, Rome (Italy). E-mail: gianluca.bianchifasani@uniroma1.it

<sup>|3|</sup> **Department of Earth Sciences, Sapienza University of Rome**  
Piazzale Aldo Moro, 5, 00185, Rome (Italy). E-mail: alberto.bretschneider@uniroma1.it

---

### | ABSTRACT |

---

The Palatine Hill is among the main archaeological sites of Roman antiquity. Today, this place requires continuous care for its safeguarding and conservation. Among the main problems, slope instabilities threaten the southwestern border of the hill flanked by the *Velabrum* Valley, as also testified by historical documents. The upper part of the investigated slope is characterized by Middle Pleistocene red-brownish tuffs known as “Tufo Lionato”. The rock mass is affected by two jointing belts featuring the slope edge and its internal portion with different joint frequency and distribution. The analysis of the geometric relationship between the joint systems and the slope attitude evidenced possible planar sliding and toppling failure mechanisms on the exposed tuff cliffs. Potential rock block failures threatening the local cultural heritage were contrasted with preliminary works for site remediation. In addition, stress-strain numerical modelling verified the hypothesis of a tensile origin for the jointing belts, suggested by fracture characteristics and orientation. A first modelling was limited to the southwestern edge of the Palatine Hill and analysed the present stress-strain condition of the slope, proving the inconsistency with the observed deformation. A second modelling was extended to the Palatine-*Velabrum* slope-to-valley system to consider the role played by the geomorphological evolution of the area on the local slope dynamics during the late Pleistocene-Holocene. Results demonstrate how original conditions of slope instability, deformation and retreat along the Palatine western edge were determined by deep valley incision, and controlled by deformability contrasts within the slope. Slope instability influenced the site occupation and development during the Roman civilization, as also indicated by the remnants of retaining walls of different ages at the slope base.

---

**KEYWORDS** | Rockfall. Slope dynamics. Cultural heritage. Palatine Hill. Rome. Italy.

**INTRODUCTION**

The Palatine Hill is located in the centre of Rome along the eastern bank of the Tiber River Valley, where a main bend of the river once received tributary streams such as the Fosso Labicano, *Vallis Murciae* and *Velabrum* valleys (Figs. 1; 2A).

The geological setting of the Palatine Hill and surroundings is composed of a multilayer made by Middle Pleistocene pyroclastic units and sedimentary formations featuring the geology of the Roman area (*e.g.* Funicello and

Giordano, 2008a,b). The Palatine Hill is shaped as a squared plateau delimited by steep slopes on the western and southern edges. The western slope is flanked by the *Velabrum* Valley, an ancient and no longer existing secondary stream of the Tiber River, which is in turn delimited by the eastern slope of the Capitoline Hill. The southern edge is separated from the Aventine Hill by the *Vallis Murciae* Valley (Figs. 1; 2A). The local geomorphological setting is the result of the Middle Pleistocene-Holocene evolution of the Roman area (upper left insight in Fig. 1), that was controlled by the volcanic processes of the Albani Hills and the Sabatini complexes and by the eusthatic-controlled, fluvial

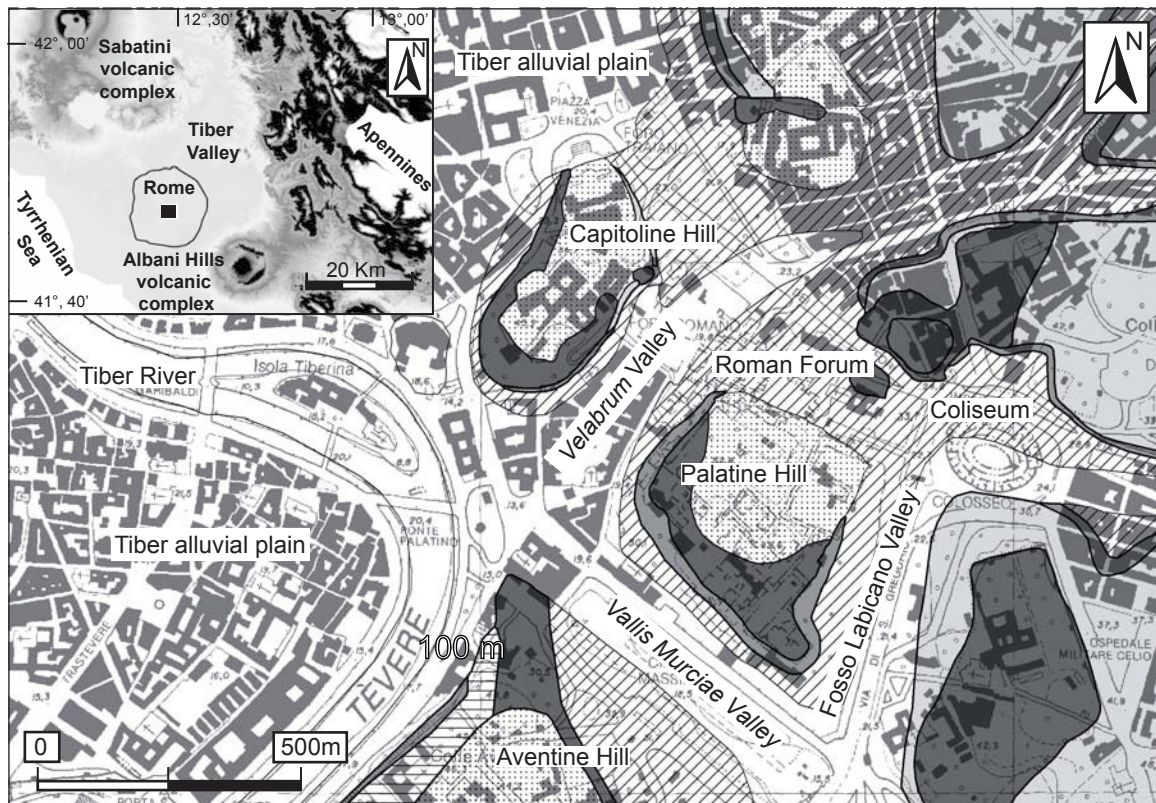


**FIGURE 1** | Map of the geological substratum in the Rome city centre on the eastern bank of the Tiber River, including the Palatine Hill (redrawn after Funicello and Giordano, 2008b). Upper left insight: geomorphological frame of the Roman area.

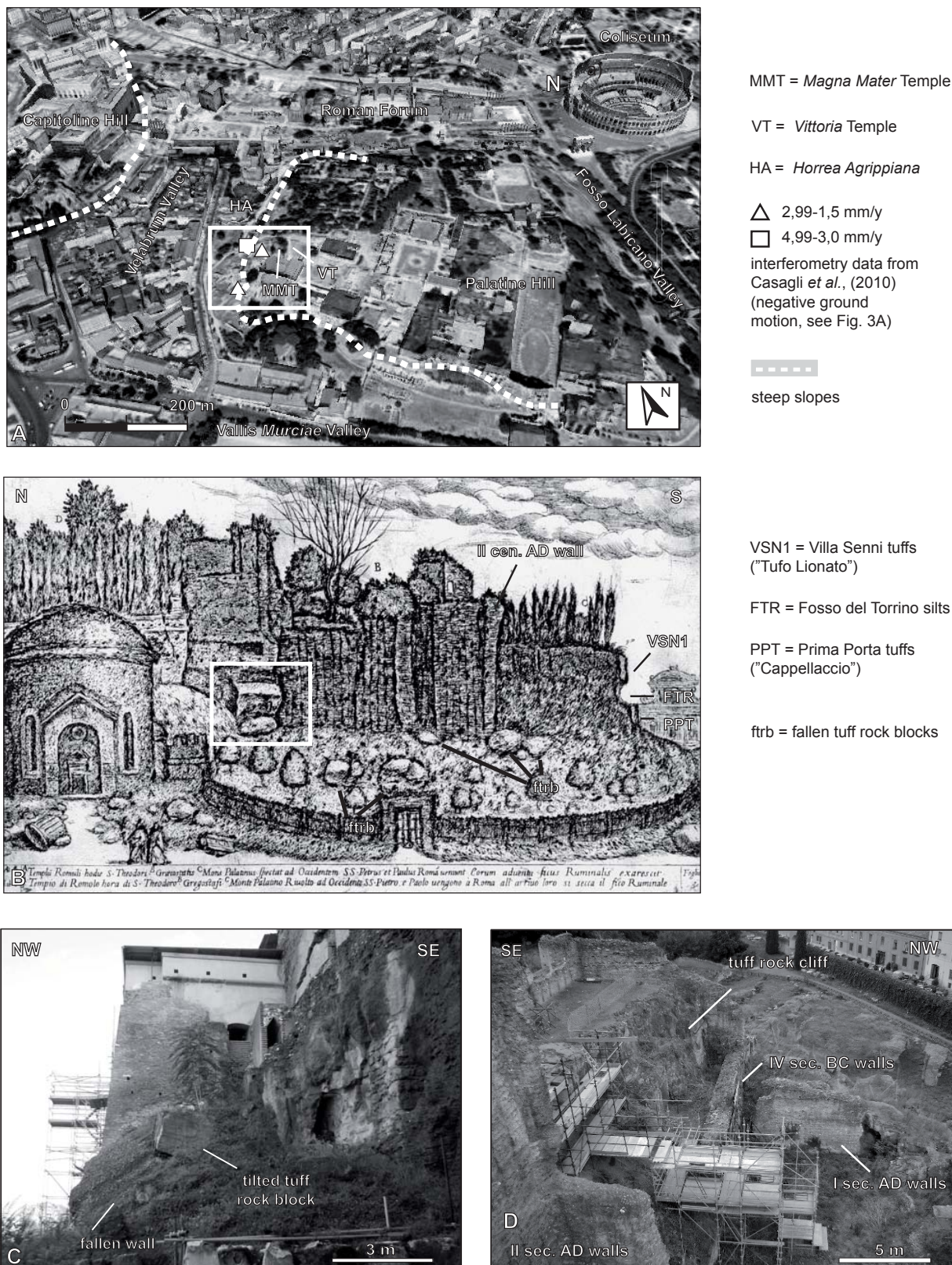


**FIGURE 2** | A) The Roman Forum-Palatine-Coliseum archaeological area in the centre of Rome (image taken from Google Earth). The white box encompasses the study area in Figure 3A; B) panoramic view of the Palatine southwestern edge in a painting of the XVIII cen. AD, showing differential erosion between tuff units and sedimentary deposits and unstable tuff rock blocks on the slope edge; C) tilted tuff rock block and fallen wall (see the white box in Fig. 2B and Fig.3A for location); D) panoramic view of the investigated slope with remnants of retaining walls of different ages.

dynamics of the Tiber River, flowing into the Tyrrhenian Sea. The sea-level regression during the Wurm period, ending with the last glacial maximum at about 20-18ka, caused a pronounced erosion of the Pleistocene multilayer carving the present fluvial drainage. In city centre areas, fluvial erosion reached the Pliocene marine bedrock of the city. The subsequent valley infilling following the sea-level rise in the Late Pleistocene-Holocene finally determined the present setting of the area (Conato *et al.*, 1980; De Rita *et al.*, 1993; Marra and Rosa, 1995; Marra *et al.*, 1995, 1998; Carboni and Iorio, 1997; Milli, 1997; Funicello and Giordano, 2008a,b). Tectonics had a limited role in the geomorphological evolution of the Palatine Hill. At the Early-Middle Pleistocene transition the main structures in the Roman area were already formed along normal faults. Very few Middle Pleistocene tectonic features characterize sectors far from the investigated site (Faccenna *et al.*, 1995; Marra *et al.*, 1995, 1998; Funicello and Giordano, 2008b). In historical times, the same area assessed different levels of damage due to several earthquakes from distant seismogenetic sources; the strongest events originated in the axial zone of the Apennine Belt (1349, 1703, 1915) and were felt in Rome with macroseismic intensities of X-XI degree of the MCS scale (Ambrosini *et al.*, 1986, Molin *et al.*, 1986; Molin and Guidoboni 1989; Tertulliani and Riguzzi 1995, Sbarra *et al.*, 2012).

Nowadays, the Palatine Hill is enclosed within the wider Roman Forum-Palatine-Coliseum archaeological area, one of the most famous and visited archaeological sites in the world (Fig. 2A). The southwestern edge of the hill was inhabited since the Iron Age (X cen. BC) until the Middle Ages (XV cen. AD); the hilltop hosts the remnants of important religious buildings dated back to the Middle Republican Age (Pensabene, 1998), such as the *Vittoria Temple* (294 BC) and the *Magna Mater Temple* (191 BC) (VT and MMT in Figs. 2A, 3A). A general frame of slope instability in this sector of the hill can be inferred from different types of evidence. Episodes of rockfalls in historical times are documented (Crocchi and Biritognolo, 1998; Pensabene, 1998) and mainly affected the jointed tuff rocks exposed in the upper part of the slope edge (Fig. 2B). Tilted rock blocks and fallen stony walls related to past events can still be observed in the study area (Fig. 2C). It is likely that these phenomena had already affected the slope during the age of Ancient Rome. The archaeological evidence of three orders of retaining walls built in the Archaic (VI cent. BC), Republican (IV cent. AD) and Early Imperial (I and II cent. AD) periods testify a long history of slope modifications (Figs. 2D; 3A). In addition, the recent elaboration of satellite interferometry data (Casagli *et al.*, 2010) has revealed negative vertical ground motion west of the *Magna Mater Temple* (Figs. 2A; 3A), in an area where the geological bedrock is exposed.

For these reasons, the local Archaeological Board commissioned a detailed analysis of the southwestern edge of the Palatine Hill to investigate the potential slope instability. If verified, this would threaten the safety of the archaeological remnants and seriously hinder any plans for the future development and fruition of the area. Several methodologies were applied at different scales of investigation. Tuff rock masses featuring two separated jointing belts in the upper part of the slope were characterised by i) geomechanical analysis and RMR classification for the determination of rock mass quality and ii) kinematic and geometric analyses (Markland's method and Hoek and Bray chart) to identify the possible failure mechanisms determining localised rock blocks instabilities. Considering the entire slope system, a 2D stress-strain modelling was initially performed to verify the consistency of the jointing belts observed in the tuff rocks with the present stress-strain conditions. In a second time, a further modelling approach analysed the local slope dynamics within the evolutionary frame of the Palatine-*Velabrum* slope-to-valley system in the Late Pleistocene-Holocene time interval (Fig. 4). This last approach allowed to test and support the hypothesis of a tensile origin for the observed jointing belts under a past stress-strain condition of the slope.

## GEOLOGICAL SETTING

### The Palatine Hill

Despite about 3000 years of human occupation and intense urbanisation, a few outcrops have been preserved along the western slope of the Palatine Hill. These outcrops allowed to reconstruct the local stratigraphic setting (Fig. 3A, B) assisted by previous studies in the same area (De Angelis-D'Ossat, 1956; Corazza *et al.*, 2004; Cavinato *et al.*, 2010; Mancini *et al.*, 2011).

The sedimentary deposits of the Santa Cecilia Formation (Fm.) form the oldest outcropping unit in the study area, also according to Funicello and Giordano (2008b). Layered, fluvio-lacustrine silts and clayey silts (with volcanic material) of this unit were observed on the cliff bordering the remnants of the *Horrea Agrippiana* (Fig. 3C), a warehouse building of the I cent. AD (HA in Fig. 2A). From the basal floor of the *Horrea Agrippiana* (13.5m asl), the Santa Cecilia Fm. reaches a thickness of about 5m. These deposits are overlain by the Palatino volcanic unit (Fig. 3B, C). This last is featured by a thin (10cm) basal layer of airfall deposits covering a paleosol and followed upwards by a lithoid, 3-m-thick, grey tuff layer with ash matrix. The Palatino unit, which originated from a pyroclastic flow from the Albani Hills at 533±5ka (Karner *et al.*, 2001), is overlain by a sequence of airfall deposits and pyroclastic rock layers

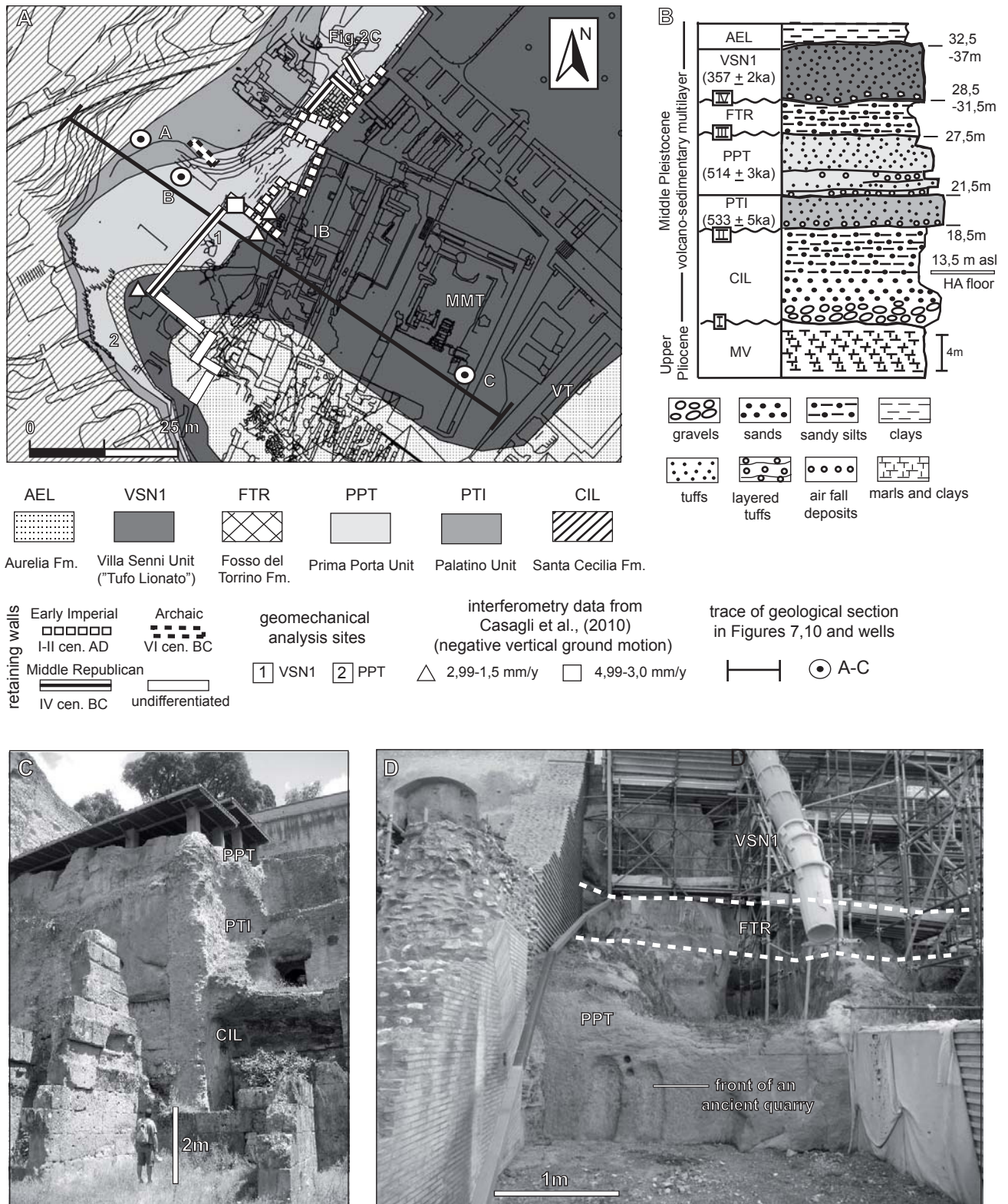


**FIGURE 3** | A) Map of the geological substratum in the southwestern edge of the Palatine Hill, underneath the anthropic deposits (redrawn after Cavinato *et al.*, 2010). MMT: *Magna Mater* Temple (III-II cen. BC); VT: *Vittoria* Temple (III cen. BC); IB: remnants of imperial buildings (I-II cen. AD); B) lithostratigraphic column: I-IV are erosive surfaces delimiting main synthematic units according to Funciello and Giordano (2008a,b). MV: Marne Vaticane Fm. (Upper Pliocene); C) outcrop at the *Horrea Agrippiana*; D) outcrop along the western slope with evidence of quarry excavation.

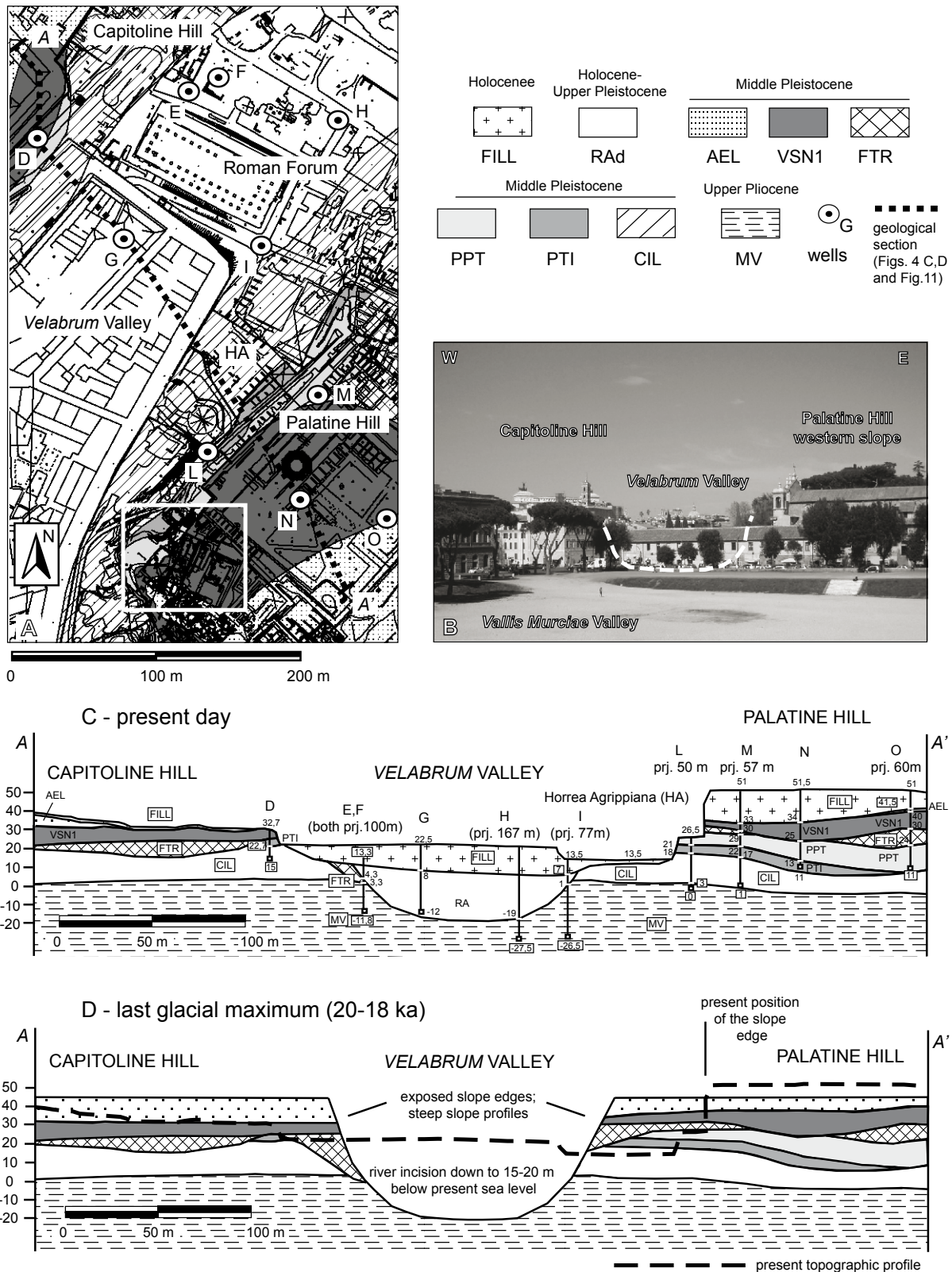


**FIGURE 4** | A) Map of the geological substratum in the Palatine-Velabrum slope-to-valley system inferred from outcrops and well data. The white box indicate the extent of Figure 3A. FILL: anthropic deposits (Holocene); RAAd: Recent Alluvial deposits (Holocene-Upper Pleistocene); for other geological units refer to legend in Figure 3A) panoramic view of the *Velabrum* Valley between the Palatine and Capitoline hills; the dashed, white line sketches the valley boundaries; C) geological cross section; D) possible reconstruction of the slope-to-valley system at the acme of the erosive process, during the last glacial maximum.

belonging to the Prima Porta volcanic unit (Fig. 3B-D), that derived instead from the Sabatini volcanic complex at  $514\pm 3\text{ka}$  (Karner *et al.* 2001). The Prima Porta unit crops out along the entire western slope of the Palatine Hill, with an average thickness of 6m (from approximately 21.5 to 27.5m asl). Archaeologists name the Palatino and Prima Porta layered, grey tuffs “Cappellaccio”. These basal tuffs are distinguished from the younger, massive, red-brownish tuffs of the Villa Senni volcanic unit (Funicello and Giordano 2008a), featuring the uppermost part of the local geological substratum and commonly known as “Tufo Lionato” (Figs. 2B; 3D; 5A, B). The “Tufo Lionato” is a pyroclastic flow erupted from the Alban Hills at  $357\pm 2\text{ka}$  (Karner *et al.*, 2001) and it is about 4-6m thick in the area. It is locally covered by the clayey and silty alluvial deposits of the Valle

Aurelia Fm. (Fig. 3A, B), that have been mainly removed from the hilltop by erosion or anthropic modifications.

Fluvio-lacustrine, yellow sandy silts are interlayered between the Prima Porta and the Villa Senni volcanic units (Figs. 3D, 5A,B). The thickness of this layer ranges from less than 1 meters to approximately 4 meters along the western edge of the Palatine Hill. This variation is due to the irregular trend of the erosive basal surface on which the Villa Senni tuffs were emplaced (surface IV in Fig. 3B). Due to their stratigraphic position, these deposits can be identified with the Middle Pleistocene Fosso del Torrino Fm. or, alternatively, with the Valle Giulia Fm. (VGU), both described in Marra *et al.* (1995; 1998) and Funicello and Giordano (2008a).

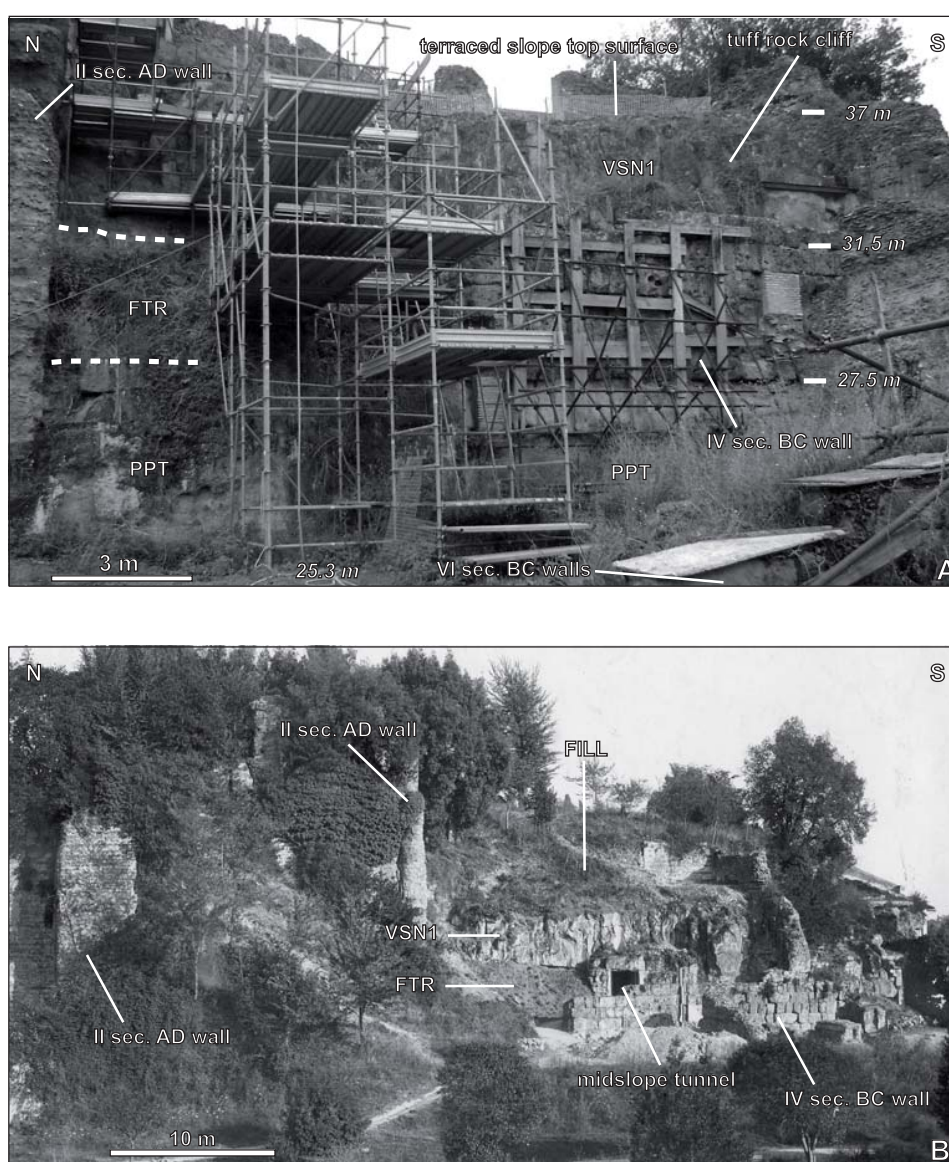


**FIGURE 5** | A) Geological setting of the investigated slope; B) panoramic view of the Palatine southwestern slope in the 30's (from the archives and with the permission of the Archaeological Board), showing also the trend of the Middle Republican (IV cen. BC) blocky wall along the slope base.

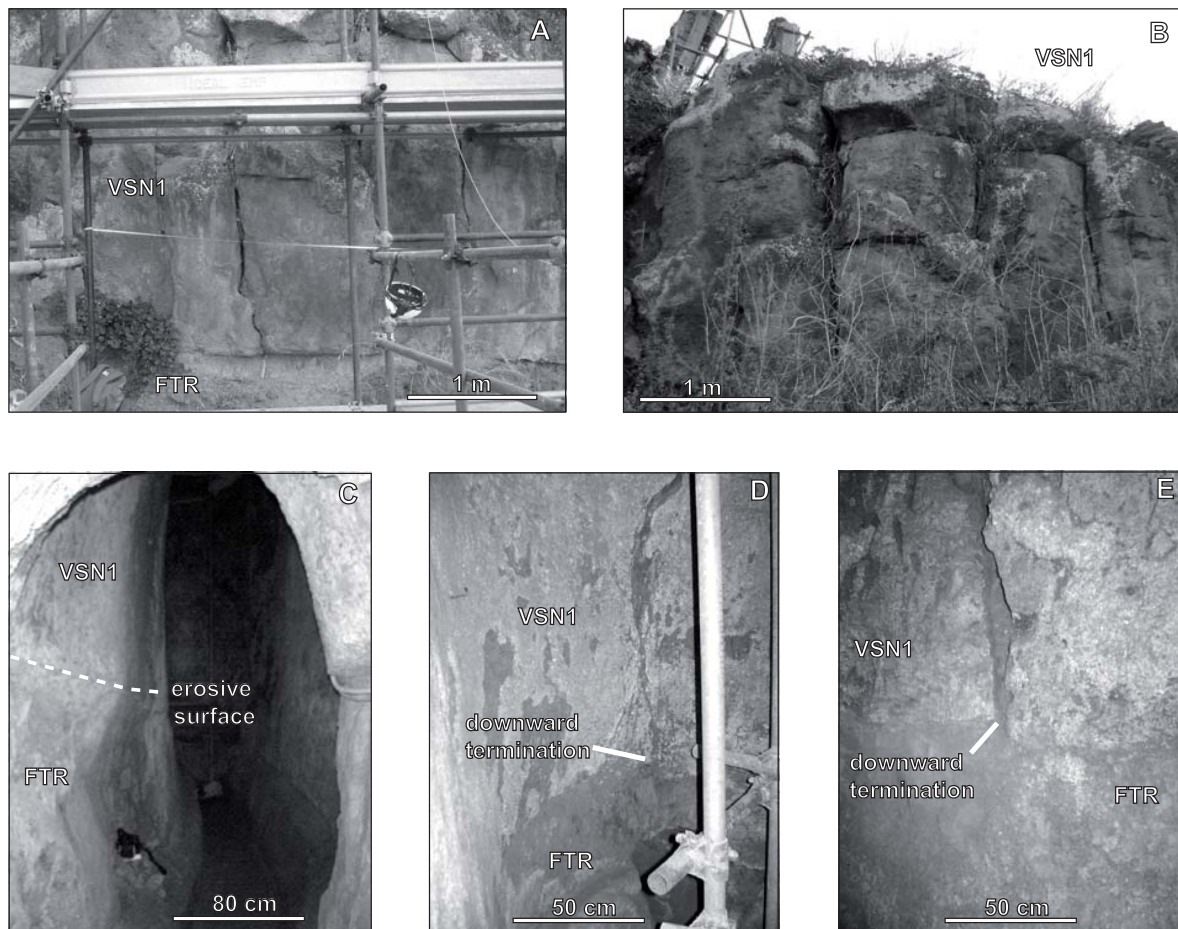


**FIGURE 6** | A), B) Jointed tuff rocks (Villa Senni unit, i.e. “Tufo Lionato”) on the upper part of the slope (external jointing belt); C) midslope tunnel (see Fig. 5B for location) excavated along the Villa Senni - Fosso del Torrino geological boundary; D) sub-vertical open fracture within the Villa Senni tuff at the end of the tunnel; E) on its left wall (internal jointing belt).

### The Palatine-*Velabrum* slope to valley system

Borehole data around and within the *Velabrum* Valley (Fig. 4A) were provided by the local Archaeological Board. Coupled with field evidence, they allowed the reconstruction of the geological setting of the *Velabrum*-Palatine slope to valley system (Fig. 4B). A geological section crossing the western slope of the Palatine Hill and reaching the eastern edge of the Capitoline Hill is illustrated in Figure 4C. It shows the sub-horizontal attitude of the Middle Pleistocene multilayer on both valley sides and the shape of the alluvial valley. The erosive basal surface of the Holocene-Upper Pleistocene alluvial deposits (mainly silts and clays with subordinate sands and basal gravels) was carved down to 15-20m below the present sea level within the Upper Pliocene Marne Vaticane Fm., this last making the geological bedrock of the entire Roman area. As aforementioned, an intense and sustained erosion occurred during the last Würm glacial period (about 116-18ka). Figure 4D

reconstructs the possible setting of the area during the acme of valley incision at the last glacial maximum (about 20-18ka); such reconstruction will be further discussed when considering the numerical modelling of the slope-to-valley system.

### SLOPE SURVEY AND GEOMECHANICAL ANALYSIS

The base of the Palatine southwestern slope is composed by a 2.2-m-thick grey tuff outcropping from an elevation of 25.3m asl and belonging to the Prima Porta volcanic unit (Fig. 5A). The grey tuff sustains the remnants of a dry-stone, blocky wall of the Middle Republican Age (IV cen. AD) and is covered by a 4-m-thick level of the Fosso del Torrino Fm. The upper part of the slope is featured by the Villa Senni tuffs, reaching a thickness of about 5m over the sandy silts. Finally, the top of the slope is a terraced surface carved within the Villa Senni tuff plate at approximately 37m asl and covered by the

anthropic layer (FILL), which includes both infilling deposits and archaeological remnants (Fig. 5A,B).

The tuff rocks exposed in the upper part of the slope are affected by jointing and moderate weathering; sub-vertical, open fractures were observed extending throughout the rock mass with a spacing between 0.4 and 1.6 m (Fig. 6A, B). This external jointing belt characterises the peripheral, 2-m-thick part of the slope. The exploration of a midslope tunnel (Fig. 5B) excavated in the proximity of the Villa Senni - Fosso del Torrino geological contact (Fig. 6C), allowed to observe an internal jointing belt characterised by vertical open fractures with a mean 3-m spacing; all these fractures are oriented sub-parallel to the slope edge and terminate downwards at the top of the Fosso del Torrino silts (Fig. 6D, E). The internal jointing belt extends between 7 and 10 metres from the tunnel entrance and is separated by the external jointing belts on the slope edge by an unjointed tuff rock zone. Inside the tunnel, it was also observed the counter-dipping ( $3^{\circ}$ -  $4^{\circ}$ ) attitude of the erosive surface separating the Villa Senni unit from the underlying Fosso del Torrino deposits (Fig. 6C). The same

surface has a horizontal to gently dip-sloping attitude on the slope edge.

Figure 7 reassumes main evidence and data collected during field survey. The geomechanical log highlights the fractures distribution in the two jointing belts. The tuff rock mass on the slope edge was characterised by means of a geomechanical analysis for the characterization of the joint systems and the determination of the rock mass quality. Dip/dip direction measurements on discontinuities were taken on both the Villa Senni and the Prima Porta units (see site locations in Fig. 3A). Data were plotted on stereo nets and then main joints sets were evidenced by box analysis (Fig. 7). The reduced amount of data collected (approximately 70 measurements) was due to the limited size of outcrops. Five joint sets were distinguished within the Villa Senni outcrop and three within the Prima Porta outcrop (Table 1). The Villa Senni tuff rocks are affected by two main joint sets, one sub-parallel to the slope edge (set 3) and the other slightly oblique (set 1). Apart set 5, all joint sets feature

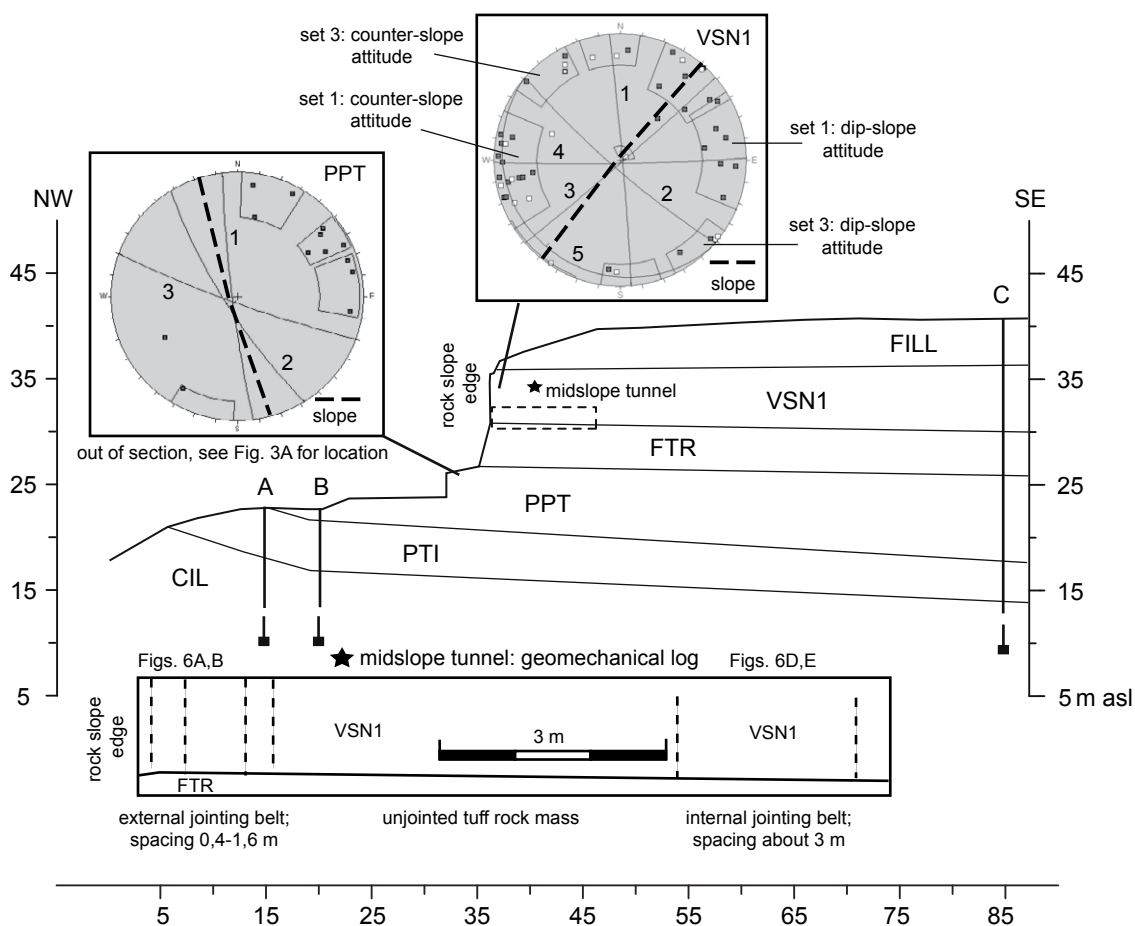


**FIGURE 7** | Cross section through the Palatine southwestern slope (trace and wells location are shown in Fig. 3A). Joint data and field observation are reported. Stereo plots for the Villa Senni and Prima Porta tuffs show main joint sets as indicated by box analysis (see also Table 1). The geomechanical log illustrates joint distribution and spacing within the midslope tunnel.

**TABLE 1** | Dip/dip direction and characteristics of main joint sets within the Villa Senni and Prima Porta tuff rock masses. JRC: Joint Roughness Coefficient

| Villa Senni unit (VSN1). Slope 88/308 |                       |             |            |              |                 |  |
|---------------------------------------|-----------------------|-------------|------------|--------------|-----------------|--|
| Joint set                             | dip/dip direction (°) | spacing (m) | length (m) | opening (mm) | roughness (JRC) |  |
| 1                                     | 89/87                 | 0.4         | 1-3        | 20-60        | 8-10; 10-12     |  |
| 2                                     | 79/223                | 0.9         | 1-3        | 20-60        | 8-10; 18-20     |  |
| 3                                     | 89/142                | 1.6         | 1-3        | 20-200       | 6-8; 14-16      |  |
| 4                                     | 87/179                | 1.5         | 1-3        | 20-60        | 6-8; 16-18      |  |
| 5                                     | 6/221                 | 1.6         | 0.5-2      | 0.1-1; 6-20  | 6-8; 14-16      |  |

| Prima Porta unit (PPT). Slope 86/252 |                       |             |            |               |                 |  |
|--------------------------------------|-----------------------|-------------|------------|---------------|-----------------|--|
| Joint set                            | dip/dip direction (°) | spacing (m) | length (m) | opening (mm)  | roughness (JRC) |  |
| 1                                    | 79/263                | 1.5         | 1-4        | 60-200        | 14-16; 16-18    |  |
| 2                                    | 78/238                | 0.9         | 0.5-3      | 60-200; > 200 | 16-18; 18-20    |  |
| 3                                    | 89/200                | 0.4         | 1-4        | 60-200        | 16-18           |  |

sub-vertical, open fractures with both dip-slope and counter-slope attitude (see stereo nets in Fig. 7).

Observations were made on the same outcrops by adopting a scan-line surveying strategy for determining the spacing, length, roughness, opening, infilling materials, weathering and hydraulic conditions of the joint systems and surfaces (Bieniawski, 1989). The open fractures are partially filled by clay material derived from moderate weathering on tuffs (soft filling). The Uniaxial Compressive Strength values for the Villa Senni and Prima Porta rock masses were estimated by an L-type Schmidt hammer (Poole *et al.*, 1980; Katz *et al.*, 2000). All data are reported in Tables 1 and 2. Data collected were used to determine the rock mass quality in agreement with the Rock Mass Rating classification by Bieniawski (1989). The basic RMR (RMRb) was calculated separately for each joint set, determining a mean RMRb values for the Villa Senni and Prima Porta outcrops of 69.4 and 76, respectively. It follows that the rock masses can be classified as good rock and very good rock (Table 2). The lower RMRb value of Villa Senni is due to the higher number of joint sets with minor spacing.

## KINEMATIC AND GEOMETRIC ANALYSIS OF THE VILLA SENNI TUFF ROCKS

### Markland method

To investigate the compatibility of joint sets with different failure mechanisms, the Markland method of kinematic analysis was applied (Markland, 1972). This analysis was limited to the external jointing belt in the upper tuff unit (Villa Senni), considering the highest number of joint sets and the position on the upper part of the slope. For this purpose, a residual friction angle  $\phi_r=30^\circ$  for a generic

weathered joint surface filled with soft material in the Villa Senni tuff rocks was adopted, in agreement with values in the literature for similar lithologies (Barton, 1974; Hoek and Bray, 1981). In the study area, the elevated value of the slope angle ( $88^\circ$ ) induces a kinematic compatibility with planar sliding on some discontinuities of joint sets 3 and 1. Sliding can occur when joint dip direction is similar to that of the slope edge (dip slope attitude), and the dip angle is lower than the dip of the slope face (Fig. 8A, A'). However, when the sub-vertical discontinuities of joint set 3 (and, subordinately, of joint set 1) are counter-dipping (reverse slope attitude), toppling may occur; in this case, fractures of joint sets 2 and 4 act as lateral kinematic boundaries for isolated rock blocks (Fig. 8B, B'), with a spacing ranging from 0.9 to 1.5m (Table1). Finally, wedge sliding processes can be excluded because of the sub-horizontal attitude of the intersection lines between sub-vertical joint surfaces.

### Possible failure mechanisms

The results of the kinematic slope analysis indicated a compatibility with planar sliding and toppling processes for some of the joint sets observed within the Villa Senni rock mass. In addition, instability conditions of isolated tuff rock blocks were verified by means of the Hoek and Bray (1981) chart, where block sliding or toppling depends on several factors including geometric parameters, as it follows:

i) block aspect ratio  $b/h$  ( $b$ =base length,  $h$ =height); ii) dip angle of the basal surface ( $\beta$ ); iii) residual friction angle along discontinuities ( $\phi_r$ )

The geometric model of Fig. 9A illustrates the shape, dimension and attitude of the jointed rock blocks on the slope edge (external jointing belt). Note that the main joint sets 2 and 4 are perpendicular and oblique to the slope section, respectively, and are therefore not represented. To

evaluate the conditions necessary for the sliding or toppling of rock blocks on inclined basal surfaces, different failure models were considered in the diagram by Hoek and Bray (1981) (Fig. 9B,C):

i) in the first failure model (toppling I), rock blocks are bounded by the reverse-slope fractures of joint sets 3 or 1, for which the Markland test revealed a kinematic compatibility with toppling. In both cases, the rock blocks stand on a basal surface corresponding to the Villa Senni - Fosso del Torrino boundary, which locally shows a dip-slope attitude ( $3^\circ$ ) on the slope edge. It follows (Fig. 9C) for set 3 that  $h=H=4.5\text{m}$ ,  $b=1.6\text{m}$  (joints are sub-vertical and

thus the block base lengths are considered equal to the joint mean spacing in Table 2) and  $b/h=0.35 > \text{tg}\beta_1(3^\circ)=0.05$ . For set 1,  $h=H=4.5\text{m}$ ,  $b=0.4\text{m}$ , and  $b/h=0.09 > \text{tg}\beta_1(3^\circ)=0.05$ . Therefore, despite the kinematic compatibility with toppling, the chart in Figure. 9B shows how large rock blocks (about  $7\text{-}11\text{m}^3$ ) bounded by the discontinuities of set 3 and overlying the Villa Senni - Fosso del Torrino limit would result stable. However, toppling may occur for the thin rock blocks (about  $2\text{-}3\text{m}^3$ ) delimited by fracture planes of set 1 (see also Fig. 8B');

ii) in the second failure model (toppling II), the basal surface is identified with the low-angle discontinuities

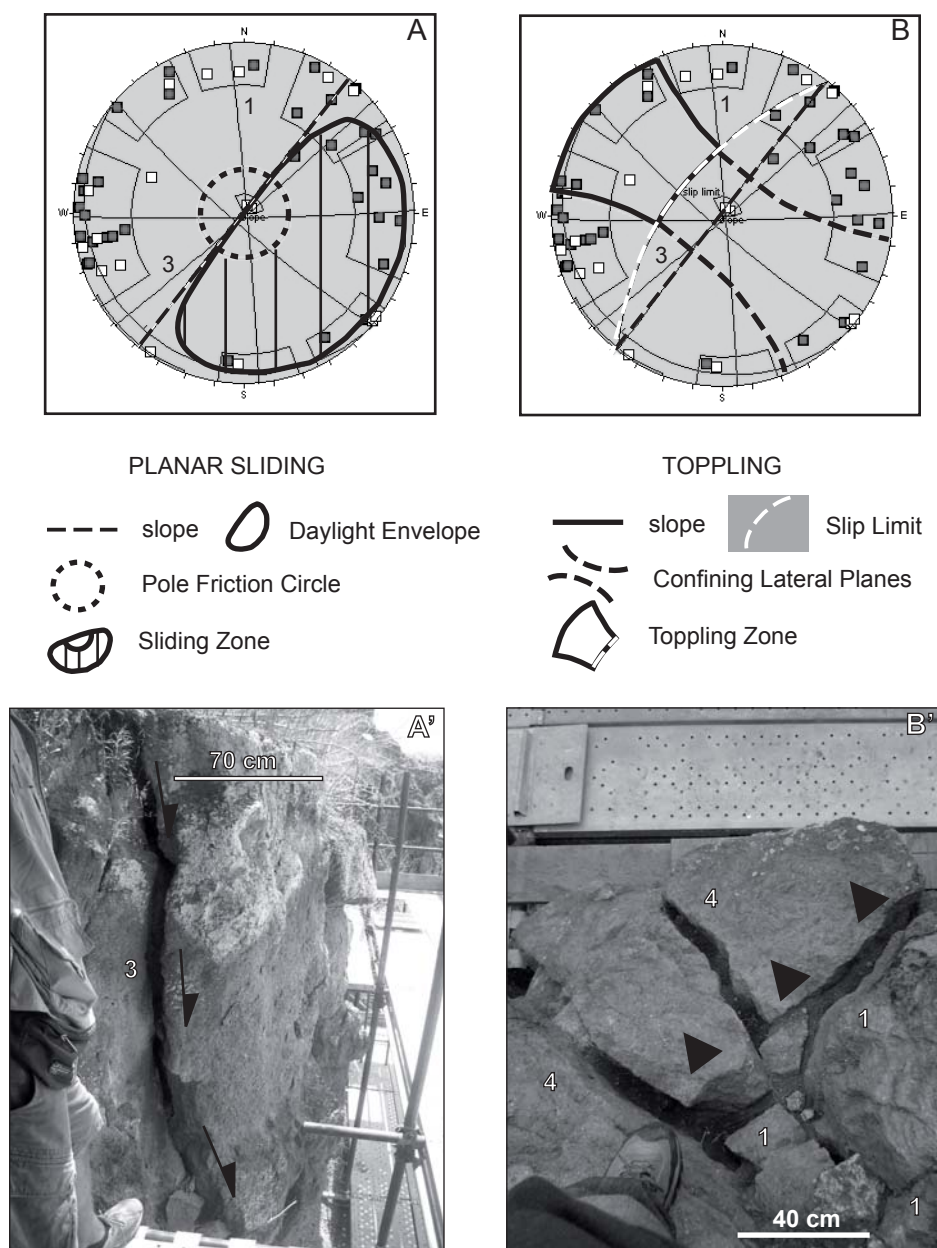
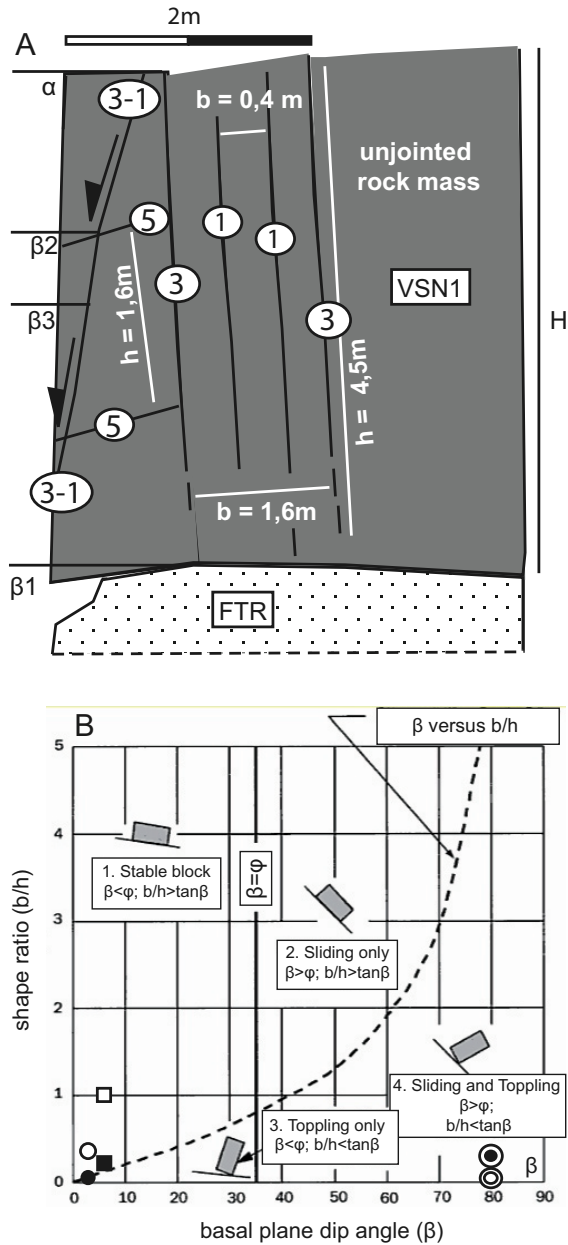


**FIGURE 8** | Results of the Markland analysis on the Villa Senni tuff rock mass for: A-A') planar sliding; B-B') toppling failure mechanisms.



$H$  = slope edge height = 4,5 m  
 $\alpha$  = slope edge dip angle = 88°  
 $h$  = rock block height (1,6-4,5 m)  
 $b$  = rock block base length (0,4-1,6 m)  
 $\beta_1$  = basal surface dip angle (VSN1-FTR boundary) = 3°  
 $\beta_2$  = basal surface dip angle (Joint set 5) = 6°  
 $\beta_3$  = basal surface dip angle (Joint set 3-1, dip slope)  $\approx$  80°  
 $\varphi$  = residual friction angle along joint = 30°

**C Possible block failure models**

**first failure model (toppling I)**

- set 3, reverse-slope attitude.  
Basal surface = VSN1-FTR limit (dip angle  $\beta=3^\circ$ ):  
 $\beta_1 < \varphi$  e  $b/h = 1,6\text{m}/4,5\text{m} = 0,33 > \text{tg}\beta(3^\circ) = 0,05$
- set 1, reverse-slope attitude.  
Basal surface = VSN1-FTR limit (dip angle  $\beta=3^\circ$ ):  
 $\beta_1 < \varphi$  e  $b/h = 0,4\text{m}/4,5\text{m} = 0,09 > \text{tg}\beta(3^\circ) = 0,05$

**second failure model (toppling II)**

- set 3, reverse-slope attitude.  
Basal surface = Joint set 5 (dip angle  $\beta=6^\circ$ ):  
 $\beta_2 < \varphi$  e  $b/h = 1,6\text{m}/1,6\text{m} = 1,0 > \text{tg}\beta(6^\circ) = 0,1$
- set 1, reverse-slope attitude.  
Basal surface = Joint set 5 (dip angle  $\beta=6^\circ$ ):  
 $\beta_2 < \varphi$  e  $b/h = 0,4\text{m}/1,6\text{m} = 0,25 > \text{tg}\beta(6^\circ) = 0,1$

**third failure model (sliding)**

- ⊙ set 3, dip-slope attitude (dip angle  $\beta_3=80^\circ$ ):  
 $\beta_3 > \varphi$  e  $b/h = (1,6/4,5=0,35 < \text{tg}\beta(80^\circ)=5,67$
- ⊙ set 1, dip-slope attitude (dip angle  $\beta_3=80^\circ$ ):  
 $\beta_3 > \varphi$  e  $b/h = (0,4/4,5=0,09 < \text{tg}\beta(80^\circ)=5,67$

**FIGURE 9** | A) Geometric model of the jointed Villa Senni rock mass on the slope edge (external jointing belt); B) chart by Hoek and Bray (1981) illustrating relationship among shape ratio ( $b/h$ ) of tuff rock blocks, dip angle of possible basal surfaces ( $\beta$ ) and residual friction angle along discontinuities ( $\varphi$ ); C) possible block failure models.

belonging to the main joint set 5 and rock blocks are again delimited by joint set 1 and 3. It follows for set 3 that  $h=1.6\text{m}$ ;  $b=1.6\text{m}$ , and  $b/h=1.0 > \text{tg}\beta_2(6^\circ)=0.05$ . For set 1,  $h=1.6\text{m}$ ,  $b=0.4\text{m}$  and  $b/h=0.25 > \text{tg}\beta_2(6^\circ)=0.05$ . Similar to the first failure model, the toppling of rock blocks delimited by the discontinuities of set 3 is prevented by the reduced inclination of the basal surface, whereas toppling of the rock blocks delimited by fractures of set 1 are on the boundary between a stable and an unstable condition.

iii) the third failure model (sliding) considers as basal surfaces those fracture belonging to joint sets 3 and 1 having a dip-slope attitude. The Markland test evidenced a kinematic compatibility with sliding processes along these discontinuities (Fig. 8A, A'). Considering a common mean dip angle of 80°, other geometric parameters are (Fig. 9C):  $h=4.5\text{m}$ ,  $b=1.6\text{m}$  and  $b/h=0.35 < \text{tg}\beta_3(80^\circ)=5.67$  for blocks delimited by set 3;  $h=4.5\text{m}$ ,  $b=0.4\text{m}$  and  $b/h=0.09 < \text{tg}\beta_3(80^\circ)=5.67$  for blocks delimited by set 1. In both cases rock blocks

**TABLE 2** | RMR classification for the Villa Senni and Prima Porta tuff rock masses. UCS: Uniaxial Compressive Strength; Jv: Joint Volumetric Index; RQD: Rock Quality Design; MSP: Mean Spacing; DC: Discontinuity Conditions; RMRb: basic Rock Mass Rating; GSI: Geological Strength Index

| RMR for the Villa Senni unit (VSN1) |                   |        |                        |        |                 |        |     |        |     |        |      |      |                    |
|-------------------------------------|-------------------|--------|------------------------|--------|-----------------|--------|-----|--------|-----|--------|------|------|--------------------|
| Set                                 | P1 (UCS)<br>(MPa) | rating | P2 (Jv;RQD)<br>(m-1;%) | rating | P3 (MSP)<br>(m) | rating | P4  | rating | P5  | rating | RMRb | GSI  | Class              |
| 1                                   | 36                | 4      | 5.4; 96.9              | 20     | 0.4             | 10     | DC4 | 17     | dry | 15     | 66   | 61   | II - good rock     |
| 2                                   | 36                | 4      | 5.4; 96.9              | 20     | 0.9             | 10     | DC4 | 15     | dry | 15     | 64   | 59   | II - good rock     |
| 3                                   | 36                | 4      | 5.4; 96.9              | 20     | 1.6             | 15     | DC4 | 16     | dry | 15     | 70   | 65   | II - good rock     |
| 4                                   | 36                | 4      | 5.4; 96.9              | 20     | 1.5             | 15     | DC4 | 17     | dry | 15     | 71   | 66   | II - good rock     |
| 5                                   | 36                | 4      | 5.4; 96.9              | 20     | 1.6             | 15     | DC5 | 22     | dry | 15     | 76   | 71   | II - good rock     |
| mean                                |                   |        |                        |        |                 |        |     |        |     |        | 69.4 | 64.4 | II - good rock     |
| RMR for the Prima Porta unit (PPT)  |                   |        |                        |        |                 |        |     |        |     |        |      |      |                    |
| Set                                 | P1 (UCS)<br>(MPa) | rating | P2 (Jv;RQD)<br>(m-1;%) | rating | P3 (MSP)<br>(m) | rating | P4  | rating | P5  | rating | RMRb | GSI  | Class              |
| 1                                   | 24                | 2      | 4.3; 100               | 20     | 1.5             | 21     | DC4 | 15     | dry | 15     | 73   | 68   | I - very good rock |
| 2                                   | 24                | 2      | 4.3; 100               | 20     | 0.9             | 23     | DC4 | 21     | dry | 15     | 81   | 76   | I - very good rock |
| 3                                   | 24                | 2      | 4.3; 100               | 20     | 0.4             | 21     | DC4 | 16     | dry | 15     | 74   | 69   | I - very good rock |
| mean                                |                   |        |                        |        |                 |        |     |        |     |        | 76   | 71   | I - very good rock |

are prone to planar sliding, eventually evolving into toppling (Fig. 9B).

## NUMERICAL MODELLING

A tensile origin for joints within the Villa Senni tuffs can be hypothesized, on the basis of several clues:

i) the presence of joint sets with orientation parallel to the slope edge; ii) the joints downward termination on the Fosso del Torrino sandy silts; iii) the presence of deformability contrasts for overlapped lithologies; iv) the lack of a confining, lateral pressure.

The main causes of joints development could be the slope retreat resulting from valley incision, slope instabilities due to differential erosion (Fig. 5B), or even slope excavations for blocks undermining (Fig. 3D). Nevertheless, the role of each one of these factors cannot be inferred nor quantified.

To verify the stress-strain congruency of the tensile origin, numerical modelling was carried out by the FDM (*i.e.* finite difference method) code FLAC 7.0 (Itasca, 2011). Two approaches were followed: the first one considered only the southwestern slope of the Palatine Hill, the second one analyzed the local slope dynamics in the wider context of the Palatine-Velabrum slope-to-valley system.

### Main remarks on modelling construction

Modelling was built taking strictly into account the geological setting of the area and the mechanical properties of tuff units and sedimentary deposits. Furthermore, in

both models the stress-strain conditions were reproduced from the deposition of the Villa Senni tuff until the present configuration. The lithological types Prima Porta and Villa Senni can be considered as weak rocks due to their low UCS value (Bieniawski, 1989, see Table 2). These materials were treated as a continuum, because jointing mainly affects the external slope portion whereas the inner portion is unjointed or with a small number of discontinuities (Fig. 7). Consequently, the FLAC code was chosen for its ability to analyse continuum media and detect the possible locations of tension failures.

The physical and mechanical properties of the sedimentary formations (Santa Cecilia, Fosso del Torrino, RAd) were obtained from a geotechnical characterisation recently completed in the Palatine area (Cavinato *et al.*, 2010, see Table 3) for seismic microzonation (Moscatelli *et al.*, 2012). The Fosso del Torrino natural unit weight was determined by laboratory tests. The strength data for the Villa Senni were obtained from triaxial tests (unpublished data) and deformability data from site tests (Bianchi Fasani *et al.*, 2011). For the Prima Porta and Palatino volcanic rock masses, physical and mechanical parameters were derived from the technical literature (Ottaviani, 1988 and references therein).

An appropriate constitutive law was assigned to each formation: all were characterised by an elastic-perfectly plastic constitutive law with a Mohr-Coulomb failure criterion. For the Villa Senni, Prima Porta and Palatino volcanic tuffs this law was combined with the Griffith criterion (Griffith, 1920) for the tensile stresses. Consequently, for those formations, described by a Mohr-Coulomb constitutive law, the tensile strength was computed as  $t=c \cdot \cot \phi$ , while for those described by a Mohr-Coulomb+Griffith constitutive law the tensile strength

was computed as  $t=c/2$  (Table 3). Roller boundaries were applied on both sides of the models and a fixed boundary condition was applied at the basis.

Secondary remarks about the developed engineering-geological models are:

i) the value of the natural unit weight of the anthropic layer (FILL in Table 3) is much higher than the value expected for a soil that originated from the weathering of tuff rocks. This assumption is consistent with the historical context of the site. Over centuries, Romans built several edifices in this area of the Palatine Hill using materials such as tuff blocks, clay bricks and basalt blocks. The unit weight of clay bricks and basalt blocks is higher than that of tuff blocks. At present, the ruins and pieces of these buildings constitute the FILL layer (Fig. 5B), that was included in some steps of the numerical modelling;

ii) pore pressure effects were neglected. In the study area, the main groundwater table is at an elevation of approximately 7m above sea level (De Angelis D'Ossat, 1956, Cavinato *et al.*, 2010), much lower than the elevation of the investigated slope (between 25.3 and 37m asl) and

therefore only rainwater affects the unsaturated zone. In addition, long-lasting slope deformation processes under a constant load are not seriously affected by groundwater table fluctuations;

iii) slope evolution in the Palatine area was analyzed under no significant compressive or tensile tectonic stresses, accordingly to the Quaternary evolution of the Roman area. Therefore, an at-rest stress state was considered for all lithologies in each modelling step.

### First approach: the Palatine southwestern slope

A regular square grid with an accuracy of 0.5m able to represent the geologic section of Figure 7 (86m wide and 31m high) was adopted in modelling setup. The initial stress-strain equilibrium was calculated considering the situation after the deposition of the Villa Senni tuffs. These last and the underlying geological layers were originally extended westwards to the Capitoline Hill with a sub-horizontal attitude (Fig. 4). After the initial equilibrium, the slope retreat until the present position was reproduced in four steps using a sequential approach (I-IV in Fig. 10A); the presence of the fill layer was considered in the last retreat step only.

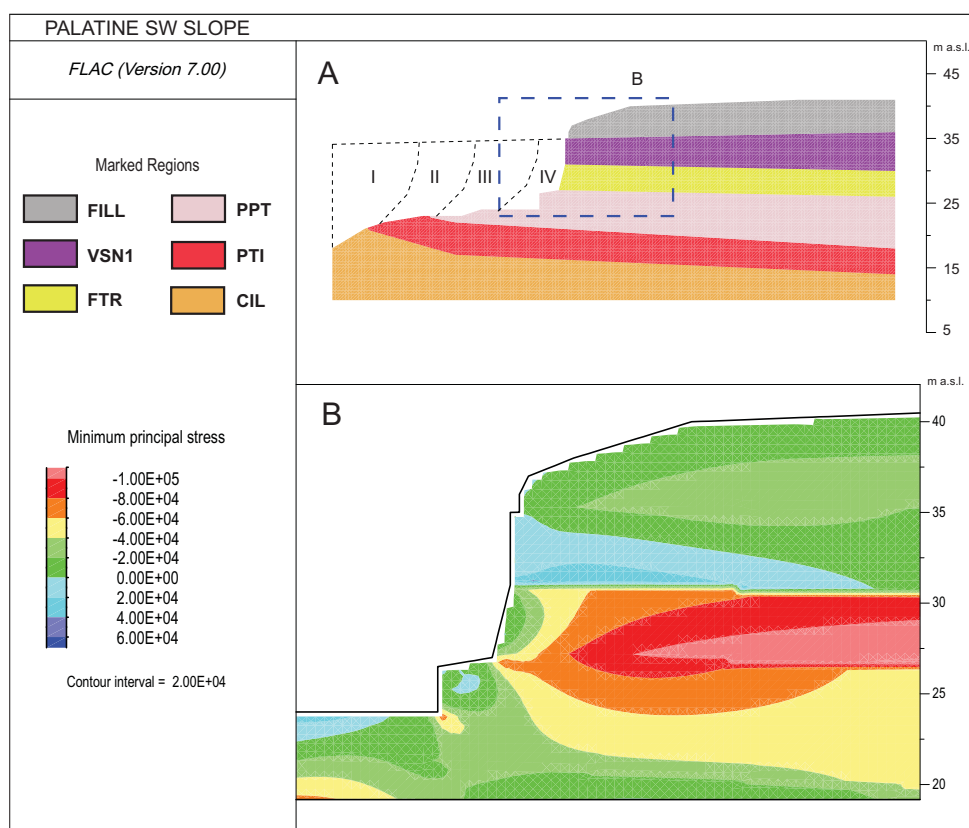


**FIGURE 10** Results of the stress-strain numerical modelling performed reproducing cross section in Figure 7 (see trace in Fig. 3A) and considering the slope evolution since the deposition of the Villa Senni unit. Geological units are distinguished by colours and codes: A) no failure or jointing is developed under the present stress-strain conditions and the slope is in a stable condition; B) plot of the minimum principal stresses nearby the slope edge: tensile stresses are positive (and light-blue coloured), compressive stress are negative.

**TABLE 3** | Physical and mechanical parameters of lithologies for numerical simulations.  $\gamma_n$ : natural unit weight; E: Young's modulus;  $\nu$ : Poisson's ratio; G: Shear modulus; K: Bulk modulus; c: cohesion; t: tensile strength;  $\varphi$ : friction angle. FILL: anthropic deposits, for the legend of other geological fms. refer to Figure 3A

|      |                       | $\gamma_n$        | E                  | $\nu$ | G                  | K                  | c                  | t                  | $\varphi$ |
|------|-----------------------|-------------------|--------------------|-------|--------------------|--------------------|--------------------|--------------------|-----------|
|      | Constitutive law      | kN/m <sup>3</sup> | Pa                 |       | Pa                 | Pa                 | Pa                 | Pa                 | (°)       |
| FILL | Mohr-Coulomb          | 20                | $1.50 \times 10^7$ | 0.30  | $5.77 \times 10^6$ | $1.25 \times 10^7$ | $5.00 \times 10^3$ | $1.07 \times 10^4$ | 25        |
| RAd  | Mohr-Coulomb          | 19                | $1.50 \times 10^7$ | 0.35  | $5.58 \times 10^6$ | $1.67 \times 10^7$ | $1.40 \times 10^4$ | $3.00 \times 10^4$ | 30        |
| AEL  | Mohr-Coulomb          | 18                | $1.50 \times 10^7$ | 0.35  | $5.58 \times 10^6$ | $1.67 \times 10^7$ | $4.00 \times 10^4$ | $8.58 \times 10^4$ | 25        |
| VSN1 | Mohr-Coulomb+Griffith | 15                | $3.00 \times 10^8$ | 0.22  | $1.23 \times 10^8$ | $1.79 \times 10^8$ | $3.20 \times 10^5$ | $1.80 \times 10^5$ | 37        |
| FTR  | Mohr-Coulomb          | 16                | $3.00 \times 10^7$ | 0.35  | $1.11 \times 10^7$ | $3.33 \times 10^7$ | $4.00 \times 10^4$ | $6.93 \times 10^4$ | 30        |
| PPT  | Mohr-Coulomb+Griffith | 12                | $3.30 \times 10^8$ | 0.20  | $1.38 \times 10^8$ | $1.83 \times 10^8$ | $3.85 \times 10^5$ | $1.75 \times 10^5$ | 42        |
| PTI  | Mohr-Coulomb+Griffith | 16                | $4.00 \times 10^8$ | 0.18  | $1.68 \times 10^8$ | $2.08 \times 10^8$ | $4.00 \times 10^5$ | $2.00 \times 10^5$ | 42        |
| CIL  | Mohr-Coulomb          | 19                | $5.00 \times 10^7$ | 0.35  | $1.85 \times 10^7$ | $5.58 \times 10^7$ | $1.40 \times 10^4$ | $3.08 \times 10^4$ | 31        |
| MV   | Mohr-Coulomb          | 21                | $4.00 \times 10^7$ | 0.25  | $1.60 \times 10^7$ | $2.67 \times 10^7$ | $1.00 \times 10^5$ | $1.73 \times 10^5$ | 30        |

Tensile strength t for materials with a constitutive law Mohr-Coulomb  $t=c \cot \varphi$ ; for materials with a constitutive law Mohr-Coulomb+Griffith  $t=c/2$

Data for CIL, FTR and RAd from Cavinato *et al.* (2010) and original laboratory tests (FTR)

Data for VSN1 from Bianchi Fazzari *et al.* (2011) and laboratory tests (unpublished data)

PPT and PTI data from Ottaviani (1988, and reference therein)

Data for AEL and MV from Ventriglia (2002) and Bozzano *et al.* (2006)

The results show that after the retreat till the present position, the slope is essentially stable (Fig. 10A). As evidenced by the distribution of minimum principal stresses (Fig. 10B) the peripheral portion of the Villa Senni tuffs is interested by tensile stresses (positive in the plot and light-blue coloured). However, these conditions do not determine the formation of tensile joints. Compressive stresses are negative and prevail in the remaining slope portion without exceeding anyhow the local strength values. Present tensile stresses are due to the deformability contrast between the Villa Senni tuffs and the Fosso del Torrino sandy silts, with a 1:1 thickness ratio.

### Second approach: the Palatine-Velabrum slope-to-valley system

The geological section (120x88m) reproduced in the second model setup by a regular square grid with an accuracy of 2m is derived from Figure 4C, D. Three cases corresponding to different geomorphological settings were simulated (Fig. 11).

Case A refers to the maximum incision of the *Velabrum* Valley at the last glacial maximum (about 20-18ka): the river had excavated into the Pliocene bedrock, but no significant alluvial deposition had started (Fig. 11A). Modelling results show that a wedge-shaped slope portion of about 30m from the valley border became unstable due to the deformation in the Santa Cecilia and Fosso del Torrino fms. Tensile fractures originated within tuff layers (Fig. 11A').

Case B considers the *Velabrum* Valley being partially filled by alluvial deposits confining the MV bedrock (consistently with E-I boreholes data in Fig. 4C). This case may correspond to the period preceding the site occupation, when the water table at the base of the Santa Cecilia deposits gave origin to several foothill springs (Pensabene, 1998). Likely, the Palatine western slope was already retreated with respect to case A, but the retreat amount is unknown. As a consequence, the same slope profile (Fig. 11B) was adopted in order to better compare modelling results. Even in this case (Fig. 11B'), a slope portion of about 30m is involved in instabilities induced by the deformation of the Santa Cecilia and Fosso del Torrino fms., but the displacement value calculated by the code for case B (2m) is about a third of case A (6m).

Case C reproduces the current situation, with the *Velabrum* Valley filled by both alluvial and anthropic deposits and the slope in its present position (Fig. 11C). The slope is in an overall stable condition (Fig. 11C'), thus confirming evidence from the first modelling (Fig. 10).

Results of the second modelling approach pointed out that slope dynamics was influenced by the stress release consequent to deep river erosion in the *Velabrum* Valley (down to the Pliocene bedrock). In addition, the deformation and retreat of the Palatine western slope (cases A and B) were controlled by the deformability contrasts given by the double overlapping of sedimentary and volcanic fms. (Palatino + Prima Porta on Santa

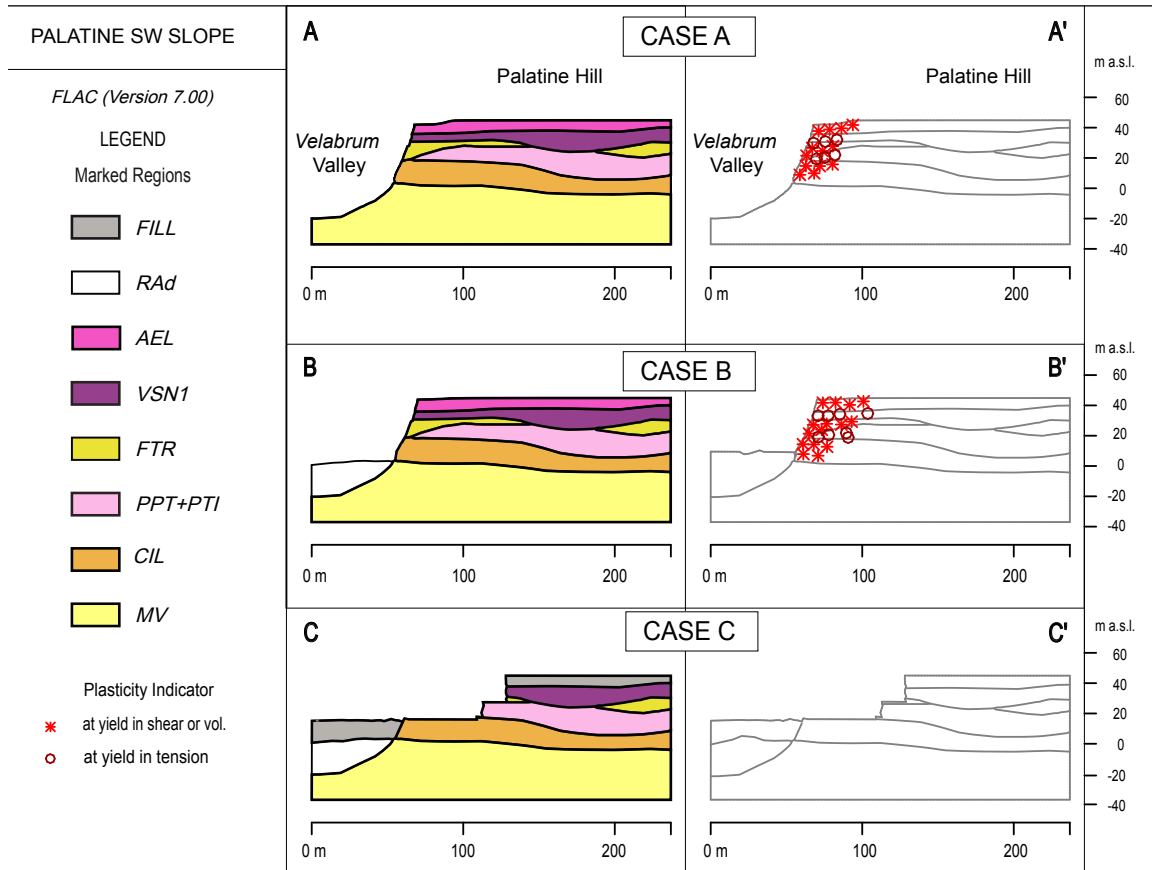


**FIGURE 11** | A) Results of the stress-strain numerical modelling reproducing part of cross-section in Figure 4 and considering the geomorphological evolution of the Palatine-Velabrum slope-to-valley system in the Late Pleistocene-Holocene: A-A') Case A, valley incision at the last glacial maximum; B-B') Case B, slope confinement by alluvial deposits; C-C') Case C, further confinement by anthropic backfill deposits.

Cecilia and Villa Senni on Fosso del Torrino). These evidences confirm the tensile origin of joints within the Villa Senni tuffs.

**DISCUSSION**

The analyses performed in this work dealt with different issues at different scales: i) the localised instabilities along the southwestern slope of the Palatine Hill, and ii) the origin of brittle deformation in jointing belts along and inside the slope.

Jointed tuff rocks were characterized by means of a geomechanical analysis and RMR classification. The UCS values and the RMR rating indicated the Villa Senni tuffs as weak rocks of very good quality. The Markland tests and the Hoek and Bray criterion applied to the external jointing belt evidenced the compatibility of some joint sets with planar sliding and toppling failure mechanisms. Although toppling is partially inhibited by the very low dip angles of the basal surfaces and the thickness of rock blocks, nevertheless it must be considered that pronounced erosion of the underlying Fosso del Torrino silts may increase

susceptibility to failures. The documented instability of the Villa Senni rock cliffs represents an elevated risk condition because rock failures may cause damage to the vulnerable, Middle Republican (IV cen. BC) retaining walls at the slope base (Figs. 2D; 5A,B). These walls represent an extraordinary witness to the site occupation and modifications. Moreover, the upper terraced surface of the Villa Senni tuff plate hosts - nearby the slope edge - important traces of the Iron Age occupation of the area (see also Fig. 12C').

To reduce risk conditions, works for site remediation were realised with the primary goal of strengthening the Villa Senni tuff rocks (Fig. 12). This goal was achieved by several operations, including a preliminary cleaning of the slope surface. Then, a 3-metres-long perforation was made with a  $\phi$  32-mm core drill in each tuff rock blocks. Rock bolts were fixed with a bicomponent, epossidic resin (Fig. 12A-A'). Afterwards, the main open fractures were cleaned and sealed with hydraulic mortar containing volcanic ashes (Fig. 12B-B'). Finally, a TiO<sub>2</sub>-based, water-proof film was spread over the slope top surface (Fig. 12C-C'). Site remediation will be completed with all the necessary technical solutions for the stabilisation of the Fosso del Torrino sandy silts.

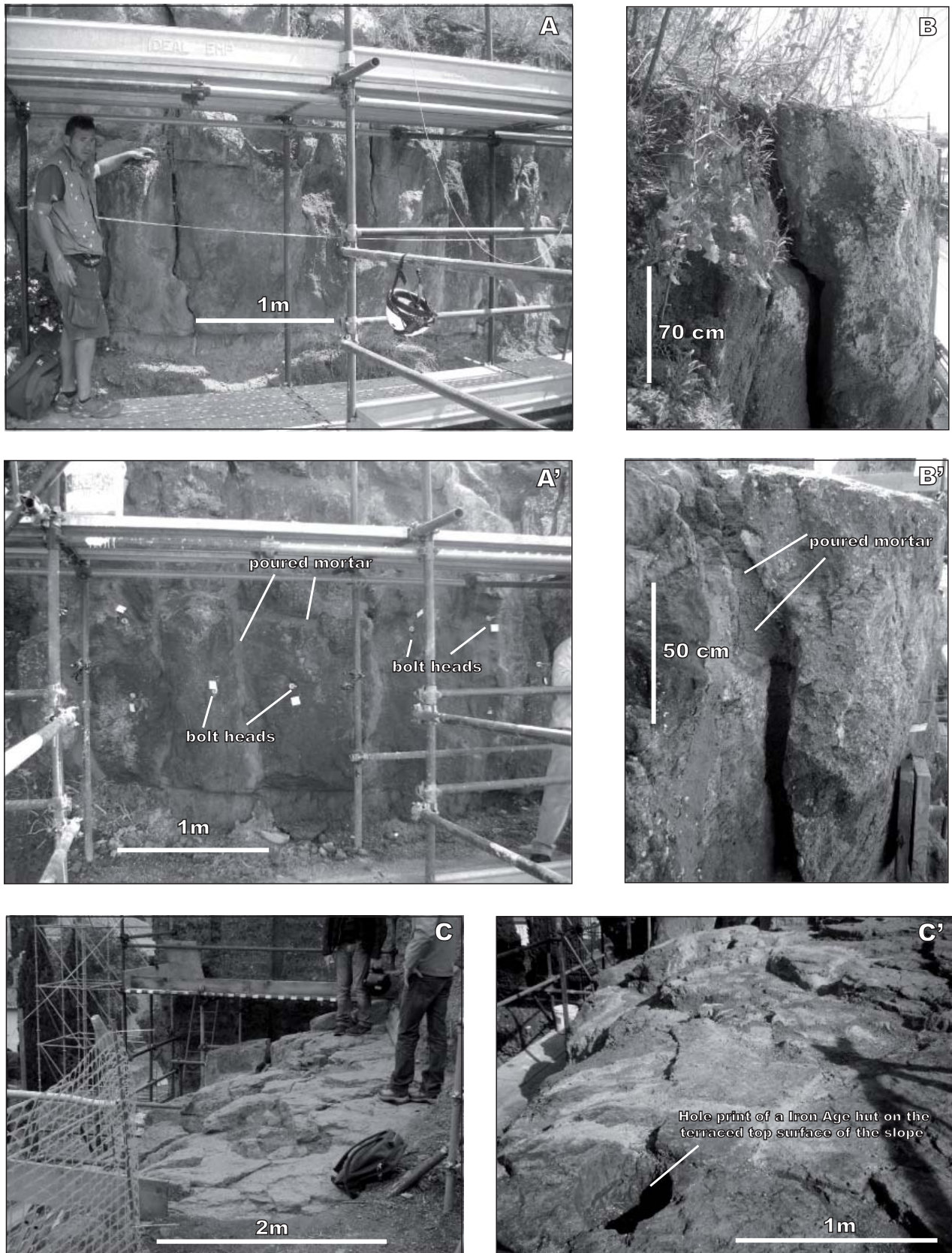


**FIGURE 12** | Site remediation works on the Villa Senni tuffs: A-A') three-meters long, stainless steel, rock bolts fixed into each rock block being potentially unstable; B-B') mortar poured within open fractures; C-C') slope top surface covered by a TiO<sub>2</sub>-based, water-proof film.

The origin of the joint sets observed on the Palatine southwestern slope was investigated in the second part of the paper by numerical modelling. The slope is made by a Middle Pleistocene multilayer characterised by deformability contrasts between volcanic tuff units and sedimentary deposits. The same geological setting is widely diffused on the Tyrrhenian side of Central Italy. Here, volcanic tuff units originated in the Middle-Upper Pleistocene are settled on Upper Pliocene-Lower Pleistocene sedimentary deposits or interfingered with coeval alluvial terrains. Under such conditions, the jointing pattern of tuff rocks outcropping on ridges, cliff slopes or isolated relieves is very often sub-parallel to the slope direction, as evidence of their tensile origin (Bozzano *et al.*, 2005; 2008). Similarly, in the Palatine area a secondary origin due to a tensile stress field can be supposed for the internal jointing belt in the Villa Senni tuffs and for some joint sets (3 and 1) in the external jointing belt. Their tensile origin is also suggested by fractures characteristics (opening and downward termination). Other joint sets could be related to other causes such as earthquakes effects from distant seismogenetic sources.

A first numerical modelling approach was performed at the slope scale and by reproducing a multiple-step process of slope retreat since the deposition of the Villa Senni tuffs (Fig. 10A). Results demonstrated how the stress distribution in the present geomorphological conditions is able to determine tensile stresses in a portion of the Villa Senni tuff rock mass (Fig. 11B), but unable to produce tuffs jointing. Apart the potential rock block failures on its edge, the slope is in an overall stability condition. Anyhow, a strength degradation of tuff rocks (for instance due to prolonged weathering) may bring to the development of tension cracks in the portion of the Villa Senni tuff plate affected by tensile strain (Fig. 10B). This has been contrasted with waterproofing of the slope top surface (Fig. 12C-C').

The tensile origin of the jointing belts within the Villa Senni tuffs is basically related to a past stress-strain state from a previous evolutionary stage of the slope. Such a conclusion is supported by the results of the second modelling approach which considered the Late Pleistocene-Holocene geomorphological evolution of a Palatine-Velabrum slope-to-valley system (Figs. 4; 11). In addition, differential erosion and anthropic excavation for blocks undermining in the Prima Porta and Palatino tuffs (Fig. 3D) can have contributed to roof instabilities in rock masses.

The deep valley erosion at the last glacial maximum determined a strong decrease of the lateral confining pressure (stress release); this modified the stress-strain conditions of the whole Palatine western slope, inducing horizontal deformations and its progressive retreat to

the present position. Rockfall episodes during alluvial deposition in the *Velabrum* Valley are testified by the presence of tuff rock blocks in boreholes drilled between the Palatine and Capitoline hills (RA, Fig. 4A) (Álvarez *et al.*, 1996; Corazza *et al.*, 2004). The progressive infilling of the valley by alluvial and anthropic deposits has progressively reduced the slope retreat until reaching stable conditions (Fig. 11).

Regarding the deformability contrasts within the Middle Pleistocene multilayer, modelling results indicate that the original 1:3 thickness ratio between volcanic units and unconfined sedimentary deposits (Santa Cecilia and Fosso del Torrino in Fig. 11A, B) was sufficient to trigger the spreading process on the unloaded slope, with the formation of tensile joints. On the contrary, the present 1:1 ratio between the Villa Senni tuffs and the Fosso del Torrino silts (Fig. 11C) does not account for the presence of tensile failures.

The occupation of the Palatine area at the beginning of the Roman civilization was certainly favoured by availability of rough materials, water supply, and its strategic position. However, this study demonstrates that site development had to face conditions of slope instability along the western edge of the hill. This is also suggested by the three lines of retaining walls partly preserved at the slope base, the most ancient dated back to the Archaic Age (VI cen BC), the others to the Middle Republican (IV cen. BC) and Early Imperial (I-II ce. AD) ages. At present, tuff rock blocks isolated by inherited, sub-vertical tensile joints are affected by gravity-driven processes determining localised slope instabilities. This condition, rather than a generalized slope instability, can justify the negative vertical ground motion indicated in the study area by interferometry data (Casagli *et al.*, 2010).

## CONCLUSIONS

A multi-methodological analysis was performed along the southwestern edge of the Palatine Hill due to concern over slope instabilities evidenced by historical documents, archaeological remnants of retaining walls, elaboration of recent interferometry data, evidence of rockfalls and jointing affecting exposed tuff rocks (Villa Senni, *i.e.* Villa Senni unit, "Tufo Lionato").

Field observations identified the presence of two jointing belts within the Villa Senni rock mass, characterised by several joint sets with sub-vertical, open fractures. Failure mechanisms such as planar sliding and toppling can occur from the external jointing belt on the slope edge. Potential rockfalls threaten elements of the local cultural heritage and may prevent the preservation and future development of

the area. A site remediation plan oriented to risk reduction was initiated with the strengthening of the tuff rock mass.

Results of a stress-strain numerical modelling reproducing the slope ruled out an overall instability of the area. Moreover, the presence of jointing belts in the Villa Senni rock masses is not consistent with the present stress-strain conditions. The origin of these fractures is related to a tensile stress state from a past evolutionary stage of the slope. This hypothesis is supported by results of a further numerical modelling reconstructing the geomorphological evolution of the Palatine-*Velabrum* slope-to-valley system from the last glacial maximum in the Late Pleistocene, onwards. The stress release determined by deep valley erosion is invoked as the main factor driving the local slope dynamics and determining the onset of tensile failures and slope retreat by progressive rockfalls. This process was controlled by the deformability contrasts within the slope. The original 3:1 thickness ratio between the volcanic units and sedimentary formations favoured slope tensile deformation, while the present, reduced 1:1 ratio inhibit the development of tensile failures. Therefore, the slope is currently only affected by gravity-driven processes.

Inherited conditions of slope instabilities, as verified in this work, hampered the site development since the beginning of the Roman civilization. This is testified by remnants of retaining walls of different ages (Archaic, Middle republican, Early Imperial) along the base of the Palatine Hill southwestern slope.

## ACKNOWLEDGMENTS

The authors are grateful to Dr. Claudia del Monti from the Archaeological Board and to Dr. Delfini who completed preliminary work for site remediation. Special thanks go to Dr. Alessandra Cicogna (CNR-ITABC) for her help in the archaeological field.

## REFERENCES

- Ambrosini, S., Castenetto, S., Cevolani, F., Di Loreto, E., Funicello, R., Liperi, L., Molin, D., 1986. Risposta sismica dell'area urbana di Roma in occasione del terremoto del Fucino del 13-1-1915. *Memorie della Società Geologica Italiana*, 35, 445-452.
- Álvarez, W., Ammerman, A.J., Renne, P.R., Karner, D.B., Terrenato, N., Montanari, A., 1996. Quaternary fluvial-volcanic stratigraphy and geochronology of the Capitoline Hill in Rome: Implications for Archeology and glacial cycles. *Geology*, 24, 751-754. DOI: 10.1130/0091-7613(1996)
- Barton, N., 1974. A review of the shear strength of filled discontinuities in rock. *Norwegian Geotechnical Institute Publication*, 105, 1-30.
- Bianchi Fasani, G., Bozzano, F., Cercato, M., 2011. The underground cavity network of south-eastern Rome (Italy): an evolutionary geological model oriented to hazard assessment. *Bulletin of Engineering Geology and the Environment*, 70(4), 533-542. DOI: 10.1007/s10064-011-0360-0
- Bieniawski, Z.T., 1989. *Engineering rock mass classifications: a complete manual for engineers and geologists in mining, civil and petroleum engineering*. New York, John Wiley and Sons Publishing, 251pp.
- Bozzano, F., Floris, M., Gaeta, M., Martino, S., Scarascia Mugnozza, G., 2005. Assetto geologico ed evoluzione per frana di rupi vulcaniche nel Lazio Settentrionale. *Bollettino Società Geologica Italiana*, 124, 413-436.
- Bozzano, F., Martino, S., Priori, M., 2006. Natural and man-induced stress evolution of slopes: the Monte Mario hill in Rome. *Environmental Geology*, 50, 505-524. DOI: 10.1007/s00254-006-0228-y
- Bozzano, F., Bretschneider, A., Martino, S., 2008. Stress-strain history from the geological evolution of the Orvieto and Radicofani cliff slopes (Italy). *Landslides*, 5, 351-366. DOI: 10.1007/s10346-010-0208-x
- Carboni, M.G., Iorio, D., 1997. Nuovi dati sul Plio-Pleistocene marino del sottosuolo di Roma. *Bollettino della Società Geologica Italiana*, 116, 435-451.
- Casagli, N., Tapete, D., Del Conte, S., Luzi, G., Fantì, R., Massaggi, S., Leva, D., 2010. Il monitoraggio satellitare e con radar da terra. In: Cecchi, R. (ed.). *Roma Archeologia: interventi per la tutela e la fruizione del patrimonio archeologico*. Milan, Mondadori Electa, 1<sup>st</sup> volume, 145-157.
- Cavinato, G.P., Moscatelli, M., Stigliano, F., Mancini, M., Bianchi, L., Cavuoto, G., Cecili, A., Cinnirella, A., Corazza, A., Di Luzio, E., Di Salvo, C., Lacchini, A., Marconi, F., Moretti, M.I., Pagliaroli, A., Piro, S., Pennica, F., Vallone, R., Verrecchia, D., Zamuner, D., 2010. Assetto geologico ed idrogeologico del Colle Palatino - Valutazione delle pericolosità geologiche. In: Cecchi, R. (ed.). *Roma Archeologia: interventi per la tutela e la fruizione del patrimonio archeologico*. Milan, Mondadori Electa, 1st volume, 84-137.
- Conato, V., Esu, D., Malatesta, A., Zarlenga, F., 1980. New data on the Pleistocene of Rome. *Quaternaria*, 22, 131-176.
- Corazza, A., Lombardi, L., Marra, F., 2004. Geologia, idrogeologia e approvvigionamento idrico del Colle Capitolino (Roma, Italy). *Il Quaternario, Italian Journal of Quaternary Sciences*, 17(2), 413-441.
- Croci, G., Biritognolo, M., 1998. Studio della stabilità e interventi di consolidamento delle strutture archeologiche e delle pendici sud-ovest del Palatino. In: Giavarini, C. (ed.). *Il Palatino. Area sacra sud-ovest e Domus Tiberiana*, Rome, Center for Information on Security Trades Central (CISTEC) Publishing, 177-194.
- De Angelis d'Ossat, G., 1956. *La Geologia del Colle Palatino in Roma. Memorie descrittive della Carta geologica d'Italia*, Servizio Geologico d'Italia, 32, 95pp.
- De Rita, D., Funicello, R., Corda, L., Sposato, A., Rossi, U., 1993. Volcanic Units. In: Di Filippo, M. (ed.). *Sabatini Volcanic*

- Complex. Consiglio Nazionale delle Ricerche (CNR), Quaderni della Ricerca Scientifica, Progetto Finalizzato Geodinamica, Monografie Finali, 114(11), 33-79.
- Faccenna, C., Funicello R., Marra, F. 1995. Inquadramento geologico strutturale dell'area romana. In: Funicello, R. (ed). La geologia di Roma. Il centro storico. Memorie descrittive della Carta geologica d'Italia, Servizio Geologico d'Italia, 50, 31-47.
- Funicello, R., Giordano, G., 2008a. La nuova carta geologica di Roma: litostratigrafia e organizzazione stratigrafica. In: Funicello, R., Praturlon, A., Giordano, G. (eds). La geologia di Roma. Dal centro storico alla periferia. Memorie descrittive della Carta geologica d'Italia, Servizio Geologico d'Italia, 80, 39-86.
- Funicello, R., Giordano, G., 2008b. Geological Map of Italy 1:50.000 scale, sheet 374 "Roma" and explanatory notes. Servizio Geologico d'Italia, Florence (Italy), Società Elaborazioni Cartografiche (S.E.L.CA.).
- Griffith, A., 1920. The phenomena of rupture and flow in solids. Philosophical Transaction of the Royal Society of London, 221, 163-198.
- Hoek, E., Bray, J.W., 1981. Rock Slope Engineering. London, The Institution of Mining and Metallurgy, 402pp.
- Karner, D.B., Marra, F., Renne, P., 2001. The History of the Monti Sabatini and Alban Hills Volcanoes: Groundwork for Assessing Volcanic-Tectonic Hazards for Rome. Journal of Volcanology and Geothermal Research, 107, 185-219. DOI:10.1016/S0377-0273(00)00258-4
- Katz, O., Reches, Z., Roegiers, J.C., 2000. Evaluation of mechanical rock properties using a Schmidt hammer. International Journal Rock Mechanics and Mining Science, 37, 723-728. DOI:10.1016/S1365-1609(00)00004-6
- Itasca consulting group, 2011. FLAC 7.0. Sapienza University of Roma, Department of Earth Science: License 213-039-0127-16143.
- Mancini, M., Moscatelli, M., Corazza, A., Pagliaroli, A., Stigliano, F., Simionato, M., Tommasi, P., Cavinato, G.P., Piscitelli, S., Marini, M., Giaccio, B., Sottili, G., 2011. Assetto geologico, idrogeologico e geotecnico dell'area archeologica comprendente il Colle Palatino, i Fori e il Colosseo. In: Cecchi, R. (ed.). Roma Archeologia: interventi per la tutela e la fruizione del patrimonio archeologico. Milan, Mondadori Electa, 2nd volume, 28-51.
- Markland, J.T., 1972. A useful technique for estimating the stability of rock slopes when the rigid wedge sliding type of failure is expected. Imperial College Rock Mechanics, Research Report, 19, 10pp.
- Marra, F., Rosa, C., 1995. Stratigrafia e assetto geologico dell'area romana. In: Funicello, R. (ed.). La geologia di Roma. Il centro storico. Memorie Descrittive della Carta Geologica d'Italia, Servizio Geologico d'Italia, 50, 49-118.
- Marra, F., Carboni, M.G., Di Bella, L., Faccenna, C., Funicello, F., Rosa, C., 1995. Il substrato plio-pleistocenico nell'area romana. Bollettino della Società Geologica Italiana, 114, 195-214.
- Marra, F., Rosa, C., De Rita, D., Funicello, R., 1998. Stratigraphic and tectonic features of the Middle Pleistocene sedimentary and volcanic deposits in the area of Rome (Italy). Quaternary International, 47-48, 51-63. DOI:10.1016/S1040-6182(97)00070-0
- Milli, S., 1997. Depositional settings and high-frequency sequence stratigraphy of the middle-upper Pleistocene to Holocene deposits of the Roman basin. Geologica Romana, 33, 99-136.
- Molin, D., Ambrosini, S., Castenetto, S., Di Loreto, E., Liperi, L., Paciello, A., 1986. Aspetti della sismicità storica di Roma, Memorie Società Geologica Italiana, 35, 439-448.
- Molin, D., Guidoboni, E., 1989. Effetto fonti, effetto monumenti a Roma: i terremoti dell'antichità a oggi. In: Guidoboni, E. (ed.). I Terremoti prima del Mille in Italia e nell'Area Mediterranea. Bologna, Storia, Geofisica Ambiente (S.G.A), 194-223.
- Moscatelli, M., Pagliaroli, A., Mancini, M., Stigliano, F., Cavuoto, G., Simionato, M., Peronace, E., Quadrio, B., Tommasi, P., Cavinato, G.P., Di Fiore, V., Angelino, A., Lanzo, G., Piro, S., Zamuner, D., Di Luzio, E., Piscitelli, S., Giocoli, A., Perrone, A., Rizzo, E., Romano, G., Naso, G., Castenetto, S., Corazza, A., Marcucci, S., Cecchi R., Petrangeli, P., 2012. Integrated subsoil model for seismic microzonation in the Central Archaeological Area of Rome (Italy). Disaster Advance, 5 (3), 109-124.
- Ottaviani, M., 1988. Proprietà geotecniche di tufi vulcanici italiani. Rivista Italiana di Geotecnica, 3, 173-178.
- Pensabene, P., 1998. Sostruzioni dell'angolo SW del Palatino: analisi delle strutture murarie. In: Giavarini, C. (ed.). Il Palatino. Area sacra sud-ovest e Domus Tiberiana. Rome, Center for Information on Security Trades Central (CISTEC), 107-154.
- Poole, R.W., Farmer, I.W., 1980. Consistency and repeatability of Schmidt Hammer rebound data during field testing. International Journal Rock Mechanics and Mining Science and Geomechanical, Abstract, 17, 167-71.
- Sbarra, P., De Rubeis, M., Di Luzio, E., Mancini, M., Moscatelli, M., Stigliano, F., Tosi, P., Vallone, R., 2012. Macroseismic effects highlight site response in Rome and its geological signature. Natural Hazards, 62, 425-443. DOI: 10.1007/s11069-012-0085-9
- Tertulliani, A., Riguzzi, F., 1995. Earthquakes in Rome during the past one hundred years. Annali di Geofisica, 38(5-6), 581-590.
- Ventriglia, U., 2002. Geologia del territorio Comune di Roma. Provincia di Roma, Servizio Geologico, Difesa del Suolo, 13 fold map, 809pp.

**Manuscript received February 2012;**  
**revision accepted September 2012;**  
**published Online April 2013.**